Hindawi
Journal of Advanced Transportation
Volume 2022, Article ID 1534815, 22 pages
https://doi.org/10.1155/2022/1534815

Research Article

Collision Avoidance Method for Autonomous Ships Based on Modified Velocity Obstacle and Collision Risk Index

Ke Zhang,[1,2] **Liwen Huang**,[1,2] **Yixiong He**,[1,2] **Liang Zhang**,[1,2] **Weiguo Huang**,[1,2] **Cheng Xie**,[1,2,3,4] **and Guozhu Hao**[1,2]

[1]*School of Navigation, Wuhan University of Technology, Wuhan 430063, China*
[2]*Hubei Key Laboratory of Inland Shipping Technology, Wuhan 430063, China*
[3]*Shaoguan Research Institute of Wuhan University of Technology, Shaoguan 512100, China*
[4]*Inland Port and Shipping Industry Research Co. Ltd. of Guangdong Province, Shaoguan 512100, China*

Correspondence should be addressed to Guozhu Hao; whuthgz@whut.edu.cn

Received 24 June 2022; Revised 13 August 2022; Accepted 1 September 2022; Published 8 October 2022

Academic Editor: Ren-Yong Guo

A novel real-time collision avoidance method for autonomous ships based on modified velocity obstacle (VO) algorithm and grey cloud model is proposed. A typical VO algorithm is used to judge whether there is a collision risk for ships in the potential collision area (PCA). Then, in order to quantify the collision risk of ships in different encounter situations within the PCA and trigger a prompt warning of danger of collision, this study sets up a novel collision risk assessment method based on asymmetric grey cloud model (AGC). It can effectively consider the randomness, ambiguity, and incompleteness of the information in the ship collision risk evaluation process. Moreover, reachable collision-free velocity sets under different encounter situations and optimal steering angle model are constructed. A real-time collision avoidance method based on modified VO algorithm and manoeuvring motion characteristics of vessels is put forward. In this model, various constraints are considered including the International Regulations for Preventing Collisions at Sea (COLREGs), ship manoeuvrability, and ordinary practice of seaman. Finally, several case studies are carried out to verify the performance and reliability of the collision avoidance model. The results show that the proposed method can not only effectively identify and quantify the collision risk in real-time but also offer proper collision-free solutions for autonomous ships.

1. Introduction

With the increasing demand for transportation worldwide, maritime transportation has witnessed a great development in the past few years [1]. At the same time, shipping traffic has become more and more intensive. The safety of ships has become the primary concern of the shipping industry [2]. As technology continues to evolve, more new technologies and tools are used to improve the safety of maritime transportation [3, 4]. However, ship accidents still occur from time to time. Figure 1 shows the causes of accidents to ships. The International Maritime Organization (IMO) report points out that more than 80 percent of maritime accidents are caused by human factors [5]. Ship collision accident is a major threat to the safety of maritime navigation, which may cause serious casualties, economic losses and marine environmental pollution, etc. [6]. Therefore, to reduce the navigational risk and casualties caused by human factors, it is very necessary to improve the ability of autonomous navigation and autonomous collision avoidance of ships. In this study, in order to solve the problem of manoeuvring to avoid collisions for autonomous ships under different encounter situations, which is an important part of the development process of autonomous ships, we propose a collision avoidance model for autonomous ships based on a modified VO algorithm and grey cloud model.

1.1. Related Works. It is of great significance to study collision risk assessment, which is the basis and precondition of ship collision avoidance. The collision risk index (CRI) is used to evaluate the probability and severity of a ship

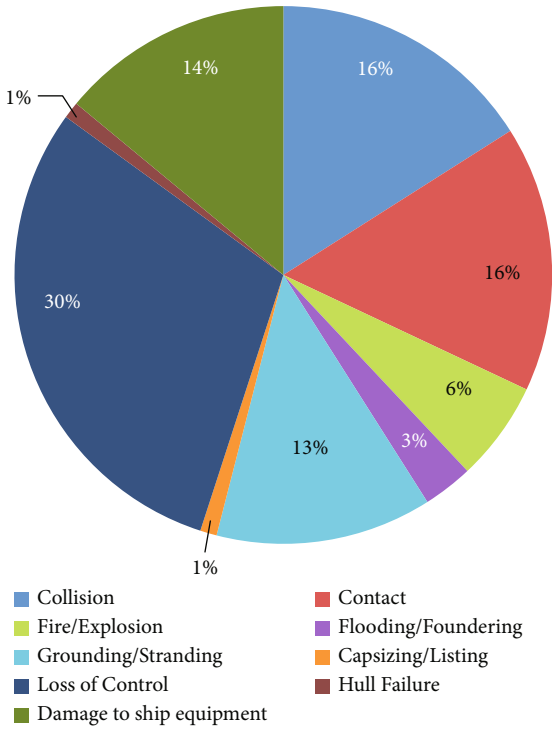

Figure 1: Causes of accidents to ships.

collision with obstacle nearby [7]. Identification and accurate quantification of CRI can help the mariners or OOW to become familiar with encounter situations and assist them in making subsequent collision avoidance decisions [8]. Zhen et al. [9] proposed the concept of ship domain, it can be used to assess the risk of ship collisions. Later, ship domain models of various sizes and shapes were proposed [10, 11]. However, these ship domain models do not consider the time dimension of ship motion information. Then, Szlapczynski and Szlapczynska first proposed the method of calculating the CRI by weighting distance to closest point of approach (DCPA) and time to closest point of approach (TCPA) parameters. Due to the inconsistent units of these factors, only relying on the two parameters of DCPA and TCPA cannot accurately assess the risk of ship collision [12]. At present, the commonly used ship collision risk assessment methods mainly include ship domain model, fuzzy theory [13], and neural networks [14]. Wang [15] developed a dynamic quaternion ship domain model that considers multiple factors such as human, ship, and navigation environment, which is suitable for open water and restricted water. In the process of designing an autonomous collision avoidance decision-making system, Wang et al. [16] used a fuzzy theory model to calculate the collision risk value and then judged the timing of the ship's avoidance action. In addition, the VO method was also used for collision risk detection. Lenart [17] first formulated the collision threat parameter area and then determined collision danger by checking whether the velocity of the ship falls into this area. Huang and van Gelder and Chen et al. [18, 19] presented various improved VO algorithms to detect multiship collision risk using historical AIS data. With the rapid development of artificial neural network (ANNs), some researchers apply ANNs to risk assessment [20]. But, due to poor generalization ability, the application of ANNs in practical marine navigation is limited, and sometimes, only the local optimum solution can be obtained. At present, the fuzzy theory is widely used in the assessment process of ship collision risk. It is recognized as the most reliable approach in the evaluation of CRI for its comprehensive consideration of DCPA, TCPA, ship speed ratio (K), distance (D), relative bearing (B), and so on. However, it is difficult to establish an accurate membership function, and the evaluation results are sensitive to the membership function, which limits the wide application of this method.

At present, there are a lot of valuable researches on collision avoidance for intelligent or autonomous ships. Ship collision avoidance technology or method can be divided into three main categories: mathematical and physical models, artificial intelligence and soft computation methods, and hybrid intelligent system, which mainly include artificial potential field (APF) [21], velocity obstacle (VO) [22–24], game theory (GT), genetic algorithm (GA) [25], artificial neural network (ANN) [26], and deep reinforcement learning (DRL) [27]. Lyu and Yin [28] proposed a novel path planning method for autonomous ships based on APF. It is suitable for ship path planning in complex navigation environment. Huang et al. [29, 30] presented a ship collision avoidance decision method based on an improved Q-learning beetle swarm antenna search algorithm and neural networks for USV. Among these algorithms, VO algorithm, as a real-time obstacle avoidance algorithm, has the advantages of simple model and fast calculation speed, which has attracted the attention of many researchers and has been widely used in the field of ship collision avoidance. Huang and van Gelder, Huang et al., and Huang et al. [18, 23, 29] applied linear VO, nonlinear VO, and probabilistic VO to ship collision prevention successively. In recent years, machine learning (ML) technology has developed rapidly. As a significant branch of machine learning, ANN and DRL have been widely used in various intelligent autonomous systems [31, 32]. Ahn et al. [33] designed an automatic collision avoidance decision-making system based on ANN-based fuzzy inference system. The automatic collision avoidance system can infer the collision risk smoothly and use the multilayer perceptual neural network and its learning process. Zhao et al. [34] constructed a novel path tracking model and collision avoidance decision model for autonomous ships based on the DRL. In addition, as a very important part of the realization of unmanned ships or autonomous ships, collision avoidance decision-making systems have received more and more attention from researchers in recent years. Many scholars have carried out research work related to the development of collision avoidance decision-making systems and achieved good results, such as collision avoidance decision-making systems and autonomous collision avoidance systems [35–37]. Nevertheless, most studies only focused on the calculation of collision-free paths. They rarely comprehensively consider COLREGs, ship manoeuvrability, ship encounter situation, and navigation practice.

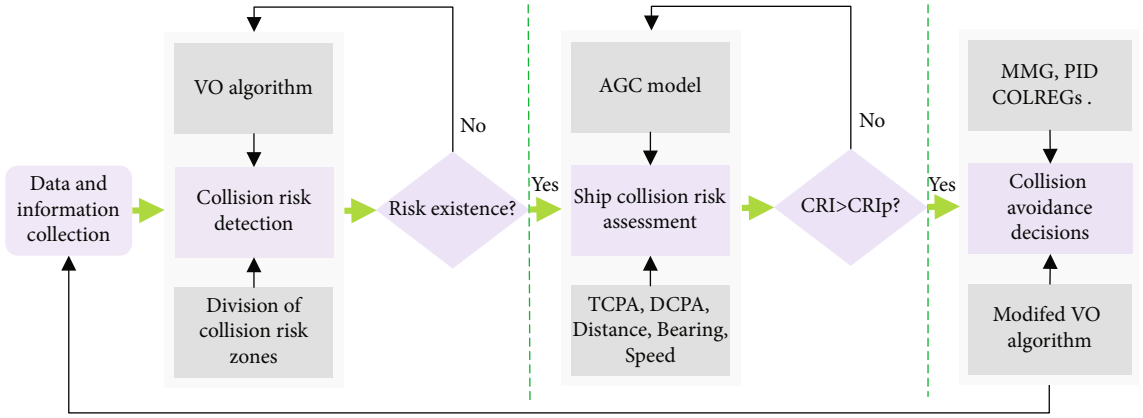

Figure 2: The framework of collision avoidance method.

Although the above-mentioned studies provide useful insights to ship collision avoidance problems, gaps between research works and reality are remaining. At present, most existing CRI models can not accurately and effectively consider the randomness, ambiguity, and incompleteness of the information in the ship collision risk evaluation process. The collision risk studies under different encounter situations are scant. For different encounter situations, there are some differences in the numerical values of the indicators that affect the collision risk. Therefore, it is necessary to construct different CRI models according to different encounter situations. In addition, few papers comprehensively consider various factors including manoeuvring motion of ships, ordinary practice of seaman, and COLREGs. In general, ships at sea are not only affected by the complex and changeable sailing environment and encounter situations but also the complex manoeuvers and movement characteristics of the ship and the constraints of COLREGs rules. In this study, we aim to solve the problem of manoeuvring to avoid collisions for autonomous ships under different encounter situations. So, we propose a collision avoidance model for autonomous ships based on a modified VO algorithm and a novel collision risk assessment model.

1.2. Motivation. The motivation of this paper is to develop a real-time automatic collision avoidance model based on the modified VO algorithm and grey cloud model. To effectively identify the ship collision risk in real time, a typical VO algorithm is used to judge whether there is a collision risk for ships in the PCA. Then, we proposed a novel collision risk assessment (CRA) method based on an AGC model. The novel CRA model integrates the actual ship encounter situation, and ship motion factors and related parameters are comprehensively considered. It can effectively consider the randomness, ambiguity, and incompleteness of the information in the ship collision risk evaluation process. Finally, a real-time collision avoidance method based on the modified VO method and manoeuvring motion characteristics of vessels is put forward. The collision avoidance model can comprehensively consider factors such as ship manoeuvrability, ship encounter situation, ordinary practice of seaman, and COLREGs, and it is especially suitable for the decision process of ship collision avoidance in coastal water. The flowchart of collision avoidance method is drawn in Figure 2.

The main contributions lie in the following aspects:

(1) A complete collision avoidance model suitable for two-ship and multiship encounter situations is developed, including collision risk detection, collision risk quantification, collision avoidance manoeuvre decision, and course control

(2) A novel collision risk evaluation model is constructed on the basis of the grey cloud model. It can effectively consider the randomness, ambiguity, and incompleteness of the information in the ship collision risk evaluation process

(3) A modified VO algorithm is developed to establish the ship collision avoidance decisions model, which comprehensively considered ship manoeuvrability, ship encounter situation, good seamanship, and COLREGs

The contents of the paper are arranged as follows: in Section 2, a novel collision risk model is proposed, which contains collision detection and collision risk evaluation. The proposed collision avoidance method is presented in Section 3, which includes ship motion model and control model, collision avoidance method, and methodology flow. The case study and analysis are carried out in Section 4. Finally, conclusions and proposals for future studies are drawn in Section 5.

2. Collision Risk Modeling

2.1. Identifying CRPs. To identify the relevant collision risk parameters (CRPs), a large number of studies regarding ship collisions risk are reviewed [7, 16, 27]. Among the studies, the variables of DCPA, TCPA, relative distance (D), relative bearing (B), and ship speed ratio (K) are selected as they are frequently mentioned in the previous studies. So, these five indicators are finally determined as assessment factors of CRI in this paper. The evaluation indicators are shown in Figure 3. The detailed calculation formula of each parameter can be found in [7].

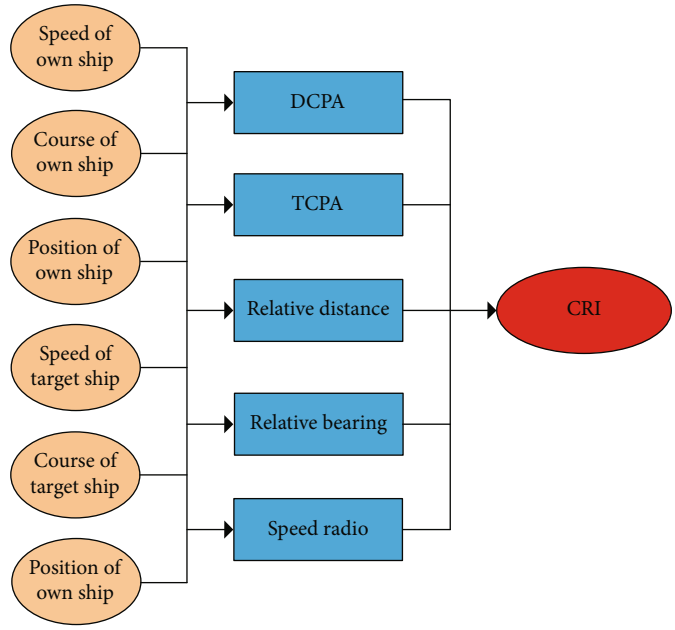

Figure 3: Influencing factors of CRI and process of calculation.

Table 1: Grade standard and grey cloud whitening weight model for CRI of head-on situation.

Risk factors	Very low	Low	Medium	High	Very high
C_1	N_L (2.8,1/3,0.01)	N_L (1.8,1/3,0.01)	N_L (1.2,0.6/3,0.01)	N_L (0.6,0.4/3,0.01)	N_L (-)
	N_R (-)	N_R (1.8,0.6/3,0.01)	N_R (1.2,0.4/3,0.01)	N_R 0.6,0.2/3,0.01)	N_R (0.4,0.4/3,0.01)
C_2	N_L (20,4/3,0.1)	N_L (16,4/3,0.1)	N_L (12,4/3,0.1)	N_L (10,2/3,0.1)	N_L (-)
	N_R (-)	N_R (16,4/3,0.1)	N_R (12,2/3,0.1)	N_R (10,2/3,0.1)	N_R (8,8/3,0.1)
C_3	N_L (5,1/3,0.01)	N_L (4,1/3,0.01)	N_L (3,1/3,0.01)	N_L (2,1/3,0.01)	N_L (-)
	N_R (-)	N_R (4,1/3,0.01)	N_R (3,1/3,0.01)	N_R (2,0.5/3,0.01)	N_R (1.5,1.5/3,0.01)
C_4	N_L (4,1/3,0.01)	N_L (3,1/3,0.01)	N_L (2,1/3,0.01)	N_L (1,1/3,0.01)	N_L (-)
	N_R (-)	N_R (3,1/3,0.01)	N_R (2,1/3,0.01)	N_R (1,0.5/3,0.01)	N_R (0.5,0.5/3,0.01)
C_5	N_L (-)	N_L (0.8,0.3/3,0.01)	N_L (1.2,0.4/3,0.01)	N_L 1.8,0.6/3,0.01)	N_L (2.2,0.4/3,0.01)
	N_R (0.5,0.3/3,0.01)	N_R (0.8,0.4/3,0.01)	N_R (1.2,0.6/3,0.01)	N_R (1.8,0.4/3,0.01)	N_R (-)

For different encounter situations, there are some differences in the numerical values of the indicators that affect the CRI. Therefore, on the basis of determining the evaluation indexes of CRI, this paper numerically defined each influencing factor (represented by C_1, C_2, C_3, C_4, and C_5, respectively) in different encounter situations and used thresholds to represent the risk grades (five states of "very low," "low," "medium," "high," and "very high"). It is important to point out that a panel of three experts are invited to provide the risk value under different encounter situations, including a captain of China Ocean Shipping Group who sails frequently in the high seas open sea, a chief officer of Jiangsu Maritime Safety Administration of People's Republic of China who is responsible for maritime search and rescue operations in the open area, and a container ship captain, running a ship to marine transport in the area for decades. For example, in the head-on situation, the value of C_4 (D) from "very high" risk to "very low" risk is 0 to 4 nm. The peak values of the five-level whitening weight function model of the indicator C_4 are 4, 3, 2, 1, and 0.5, respectively. Using Equations (1)-(3), the asymmetric grey cloud whitened weight models are calculated; they are very low (4,1/3,0.01; -), low (3,1/3,0.01; 3,1/3,0.01), medium (2,1/3,0.01; 2,1/3,0.01), high (1,1/3,0.01; 1,0.5/3,0.01), and very high (-; 0.5,0.5/3,0.01), respectively. Similarly, the index values of three encounter situations are shown in the following table. As a result, detailed information about the categories and the numerical definitions of linguistic states for three encounter situations is presented in Tables 1–3.

2.2. Collision Detection Model. Under normal circumstances, before CRI is calculated, it is necessary to judge whether the collision risk exists between the ships. If collision risk exists, it will further calculate the collision risk value and decide whether to take a collision avoidance decision. At present, most studies discuss two indicators of DCPA and TCPA in

Table 2: Grade standard and grey cloud whitening weight model for CRI of overtaking situation.

Risk factors	Very low	Low	Medium	High	Very high
C_1	N_L (3,1.0/3,0.01)	N_L (2,1.0/3,0.01)	N_L (1.5,0.5/3,0.01)	N_L (0.8,0.7/3,0.01)	N_L (-)
	N_R (-)	N_R (2,0.5/3,0.01)	N_R (1.5,0.7/3,0.01)	N_R (0.8,0.3/3,0.01)	N_R (0.5,0.3/3,0.01)
C_2	N_L (18,6/3,0.1)	N_L (12,6/3,0.1)	N_L (10,2/3,0.1)	N_L (8,2/3,0.1)	N_L (-)
	N_R (-)	N_R (12,2/3,0.1)	N_R (10,2/3,0.1)	N_R (8,3/3,0.1)	N_R (5,3/3,0.1)
C_3	N_L (3,0.5/3,0.01)	N_L (2.5,0.5/3,0.01)	N_L (2,0.5/3,0.01)	N_L (1.5,0.5/3,0.01)	N_L (-)
	N_R (-)	N_R (2.5,0.5/3,0.01)	N_R (2,0.5/3,0.01)	N_R (1.5,0.5/3,0.01)	N_R (1,1.5/3,0.01)
C_4	N_L (210,37.5/3,1)	N_L (180,37.5/3, 1)	N_L (150,30/3,1)	N_L (120,30/3, 1)	N_L (-)
	N_R (-)	N_R (180,30/3,1)	N_R (150,30/3, 1)	N_R (120,5/3, 1)	N_R (115,5/3,1)
C_5	N_L (-)	N_L (1.5,0.3/3,0.01)	N_L (1.8,0.3/3,0.01)	N_L (2,0.2/3,0.01)	N_L (2.4,0.4/3,0.1)
	N_R (1.2,0.3/3,0.01)	N_R (1.5,0.3/3,0.01)	N_R (1.8,0.2/3,0.01)	N_R (2,0.4/3,0.01)	N_R (-)

Table 3: Grade standard and grey cloud whitening weight model for CRI of crossing situation.

Risk factors	Very low	Low	Medium	High	Very high
C_1	N_L (3,1/3,0.01)	N_L (2,1/3,0.01)	N_L (1.5,0.5/3,0.01)	N_L (0.8,0.7/3,0.01)	N_L (-)
	N_R (-)	N_R (2,0.5/3,0.01)	N_R (1.5,0.7/3,0.01)	N_R (0.8,0.3/3,0.01)	N_R (0.5,0.3/3,0.01)
C_2	N_L (20,2/3,0.1)	N_L (18,2/3,0.1)	N_L (12,6/3,0.1)	N_L (8,4/3,0.1)	N_L (-)
	N_R (-)	N_R (18,6/3,0.1)	N_R (12,4/3,0.1)	N_R (8,3/3,0.1)	N_R (5,3/3,0.1)
C_3	N_L (4,0.5/3,0.01)	N_L (3.5,0.5/3,0.01)	N_L (2.2,1.3/3,0.01)	N_L (1.5,0.7/,0.01)	N_L (-)
	N_R (-)	N_R (3.5,1.3/3,0.01)	N_R (2.2,0.7/3,0.01)	N_R (1.5,0.5/3,0.01)	N_R (1,0.5/3,0.01)
C_4	N_L (100,12.5/3, 1)	N_L (90,12.5/3, 1)	N_L (67.5,22.5/3, 1)	N_L (40,27.5/3, 1)	N_L (-)
	N_R (-)	N_R (90,22.5/3, 1)	N_R (67.5,27.5/3, 1)	N_R (40,30/3, 1)	N_R (10,30/3, 1)
C_5	N_L (-)	N_L (0.8,0.3/3,0.01)	N_L (1,0.2/3,0.01)	N_L (1.5,0.5/3,0.01)	N_L (2.2,0.7/3,0.01)
	N_R (0.5,0.3/3,0.01)	N_R (0.8,0.2/3,0.01)	N_R (1,0.5/3,0.01)	N_R (1.5,0.7/3,0.01)	N_R (-)

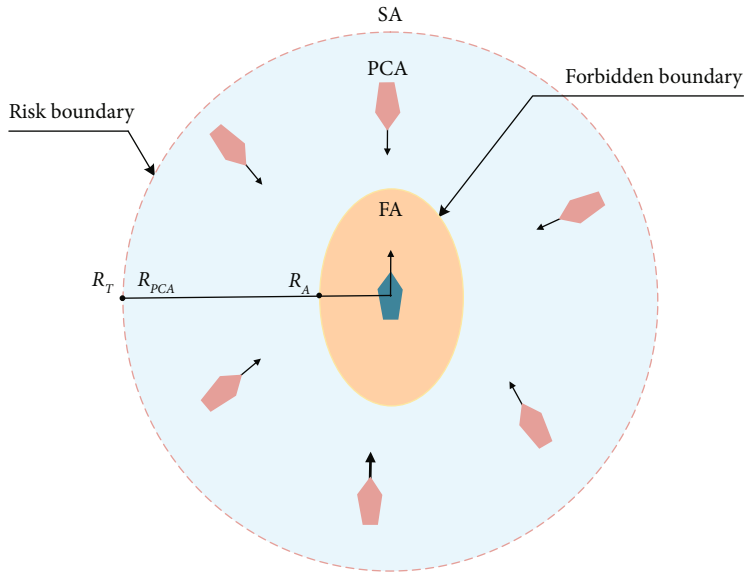

SA: Safe Area
PCA: Potential Collision Area
FA: Forbidden Area

Figure 4: Risk area around the OS.

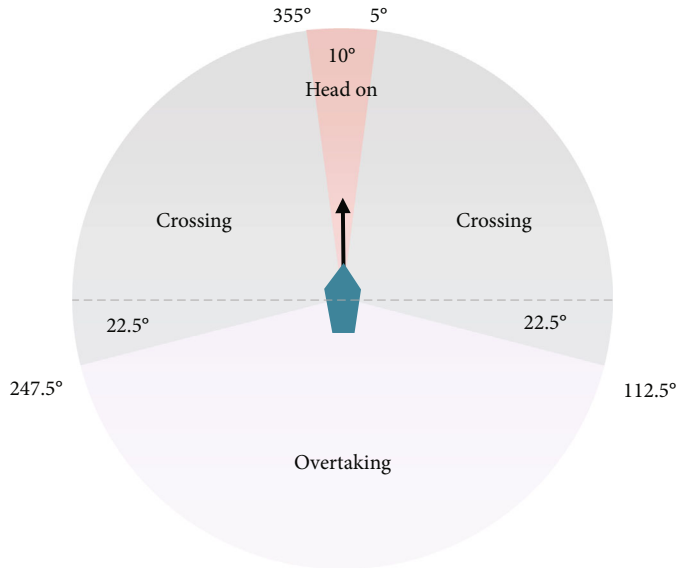

Figure 5: The classification of different ship encounter situations.

the collision detection process [38]. VO algorithm is put to wide use in robot collision avoidance and ship obstacle avoidance. According to the principle of VO, the speed sets of all ships that may cause collision risk can be calculated. If the relative speed of the two ships is not in the potential collision area, it is considered to have no collision risk. Based on it, the VO algorithm is used in this paper to determine whether there is a collision risk between OS and TS. Specific ideas are as follows: (1) obtain the speed, position, course, and relative distance of the OS and TSs through radar and AIS system. (2) Construct the velocity obstacle area according to the collision information between the OS and TSs. (3) Then, calculate the relative speed of the OS and TSs, and judge whether there is a collision risk between ships based on the relative speed falling in the relative collision cone or the absolute collision cone. The detailed process of the VO algorithm to detect ship collision risk can be found in reference [22].

Before the detection of ship collision, the ship risk area needs to be divided. It is supposed that the water area around OS is divided into three zones, namely, the forbidden area (FA, collision of entities is bound to happen), potential collision area (PCA, collision risk begins to exist and becomes apparent), and safe area (SA, no collision risk) shown in Figure 4. Other than the OS, no other ships can sail in the FA. Nevertheless, another ship would probably enter the PCA, the probability of which depends on the behavior of navigators, sailing speeds, DCPA, TCPA, and the navigational conditions of the water areas. For ships in the PCA, according to COLREGs, the encounter scenarios of two ships are classified into three situations, that is, the head-on situation, the crossing situation, and the overtaking situation. Among them, rules 13, 14, and 15 of the COLRGEs describe three encounter situations, respectively, in Figure 5.

As shown in Figure 5, R_A is the distance from the OS to the boundary of FA, and R_T is the distance between the TS and OS. R_{PCA} is the distance from the OS to the boundary of the PCA. R_{PCA} can be appropriately adjusted according to the different encounter situations. In this case, R_{PCA} is 6 nm [39]. Here, FA is equivalent to the ship domain. In this paper, the FA (ship domain) is represented by an elliptic equation. For methods introducing ship domain [10], for all encounter situation, semimajor axis is $5L$, and semiminor axis is $2.5L$, where L represents the length of the OS.

2.3. Collision Risk Assessment Model. Collision risk index (CRI) is an important reference basis for ship collision avoidance decision. For the ships in the process of navigation, the ship's officer not only needs to judge whether the two ships will collide according to the surrounding ships and environmental information but also needs to measure the possibility of collision between ships according to the degree of collision risk. Therefore, in the process of studying ship collision avoidance, to establish a scientific and accurate collision risk model is the key to the success of ship collision avoidance decision for autonomous ships. At present, scholars at home and abroad have proposed a variety of methods (such as ship domain model and fuzzy theory model) to calculate CRI. However, most existing CRI models cannot accurately and effectively consider the randomness, ambiguity, and incompleteness of the information in the ship collision risk evaluation process. Although fuzzy theory can be used to deal with the fuzzy and uncertain information of ship collision, it is very difficult to construct an accurate membership function, and the evaluation results are very sensitive to the membership function. Based on this, this paper proposes a ship collision risk assessment model based on grey cloud model.

The grey cloud model was proposed by Wang [40] by combining the theory of cloud model with the grey theory. It is an evaluation model integrating grey, randomness, and fuzziness to overcome the shortcomings of traditional whitening functions. As a multi-index evaluation system, ship collision risk assessment inevitably has the characteristics of ambiguity and randomness, and grey cloud model

integrates the advantages of grey theory and cloud theory, which can play the advantages of cloud model in dealing with randomness and fuzziness and effectively solve the problem of uncertainty information representation caused by grey factors. The grey cloud model can represent the fuzziness and randomness and also their relations of uncertain concepts, and it is suitable for dealing with uncertain information and obtaining accurate estimation. At present, it has been successfully applied in many fields such as flood disaster assessment [41], transformer status assessment, and guidance simulation system evaluation [42].

Definition. assuming that U is a domain of $U = \{x\}$, C is the language value associated with U, and the whitening weight of element x in U for the grey concept expressed by C is a random number with a stable tendency, then the distribution of whitening weight on the domain U is called grey cloud whitened weight function, which is called grey cloud for short.

The numeral characteristics of grey cloud model are characterized by peak value Cx, left and right boundary (L_x, R_x), entropy En, and hyperentropy He, respectively. Cx is the value of the whitening weight equal to 1. They have the following relationship:

$$\begin{cases} Cx = \dfrac{L_x + R_x}{2}, \\ En = \dfrac{R_x - L_x}{6}, \\ He = \dfrac{En}{\alpha}, \end{cases} \tag{1}$$

where α is any given constant.

The mathematic expectation of grey cloud model is defined by the following formula:

$$\mathrm{NGL}(x) = \exp\left[-\frac{(x - Cx)^2}{2(En)^2}\right]. \tag{2}$$

In grey cloud model, the median value of grey number is taken as the peak value Cx to maintain the symmetry of the model, which is an ideal special case (as can be seen in Figure 6). In the actual situation, when the left boundary value L_x and the right boundary value R_x are known, the peak value Cx is often not the middle value, but a value that can be arbitrarily taken in the interval $[L_x, R_x]$. This not only limits the flexibility of Cx but also affects the reliability of the assessment results. Therefore, this paper proposes the asymmetric grey cloud (AGC) model based on the grey cloud model. It can realize the flexible value selection of the digital features, which is closer to the actual situation. It not only solves the problem of information uncertainty in the evaluation process but also enhances the practicality of the model and makes the model superior. The AGC whitenization weight function is shown in Figure 6(d). Thence, in order to quantify the ship collision risk, a novel CRI model based on the AGC is proposed for different encounter situations. The realization process of the CRA model based on the AGC model is shown below.

Stage 1. AGC whitened weight function construction

Assume that there are n assessment objects, m risk factors, and k different grey classes. Construct an AGC model with the left boundary point, right boundary point, and center point value of the kth ($k = 1, 2, \cdots, n$) grey parameter N $(Ex_{NL}, En_{NL}, He_{NL}, Ex_{NR}, En_{NR}, He_{NR})$. In this paper, each risk factor and CRI value are divided into five levels (as can be seen in Tables 1–3), N is the number of target ships with collision risk, and the value of risk factors m is 5. The numerical characteristics of the grey cloud of each indicator are calculated by Formula (1). The expressions of the whitenization weight function for the AGC model can be represented as follows.

$$f_j^k(x) = \begin{cases} \exp\left[-\dfrac{(x - Cx)^2}{2(En_{NL})^2}\right], & x \in [Lx, C_x], \\ \exp\left[-\dfrac{(x - Cx)^2}{2(En_{NR})^2}\right], & x \in [C_x, Rx], \\ 0, & x \notin [Lx, Rx]. \end{cases} \tag{3}$$

Stage 2. calculate whitening weight value

In order to eliminate the error caused by the whitening weight value $f_j^k(x_{ij})$ calculated, the mean value of multiple times can be taken as the final whitening weight value, which is calculated by using the following equation:

$$f_j^k(x_{ij}) = \frac{f_{j1}^k(x_{ij}) + f_{j2}^k(x_{ij}) + \cdots + f_{jN}^k(x_{ij})}{N}, \tag{4}$$

where N denotes the calculation times and $f_{jN}^k(x_{ij})$ is the whitening weight function value of the Nth time. In this paper, we take $N = 100$.

And normalize the whitening weight value to get the final indicator AGC whitening weight value.

$$u_i^k(x_{ij}) = \frac{f_j^k(x_{ij})}{\sum_{k=1}^{s} f_j^k(x_{ij})}, \tag{5}$$

where $u_i^k(x_{ij})$ is normalized grey cloud clustering coefficient.

Stage 3. indicator weights determination

In general, indicator weights of CRI are generally determined by experts' subjective experience scoring. Some scholars [16, 27, 43] have obtained the indicator weight value of CRI by using the navigation simulator and expert experience. On the basis of referring to other research results and combining the opinions of three invited experts, this paper determined the weight coefficient of five factors, as shown in Table 4.

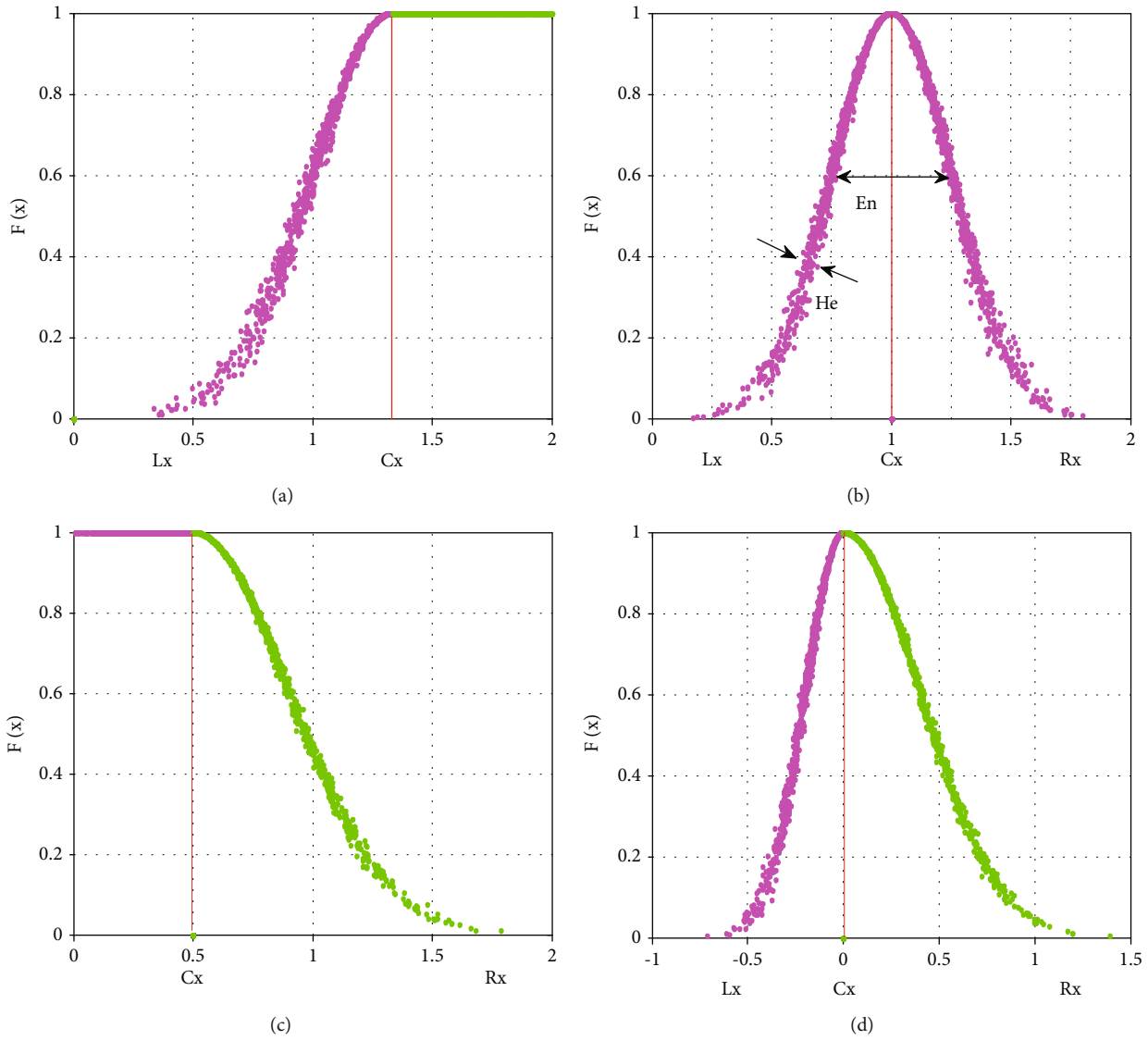

Figure 6: The grey cloud whitenization weight function. (a) The function of lower measure. (b) The function of moderate measure. (c) The function of upper measure. (d) The AGC whitenization weight function.

Table 4: Indicator weights of CRI evaluation.

Risk factors	DCPA	TCPA	D	B	K
Weight	0.400	0.367	0.140	0.060	0.033

Stage 4. grey cloud clustering coefficient calculation

Assume that the grey cloud clustering coefficients for evaluation indicator i belonging to grey class k is σ_i^k, which is defined as

$$\sigma_i^k = \sum_{j=1}^{m} u_j^k(x_{ij}) * \omega_i, \tag{6}$$

where ω_i is the weight of ith indicator.

Stage 5. determine the collision risk value

The comprehensive clustering coefficients of the evaluation object i calculated by grey cloud clustering is as follows:

$$\sigma_i^* == \max_{0\le k\le 5}\left\{\sigma_i^k\right\}, \tag{7}$$

where σ_i^* represents i object belonging to grey class of maximum value.

In general, the calculations of the above-mentioned risk values are presented by single values, which cannot reflect CRA without appropriate data transformation and normalization. Assume that $[a_i, b_i]$ $(i = 1, 2, \cdots, 5)$ is assigned to the five grade values from very low risk to very high risk excellent, respectively. Here, we give the interval values as [0,0.2], [0.2,0.4], [0.4,0.6], [0.6,0.8], and [0.8,1], respectively. Since, the maximum value of comprehensive clustering coefficients is usually distributed in the interval [0.2,0.6] [41],

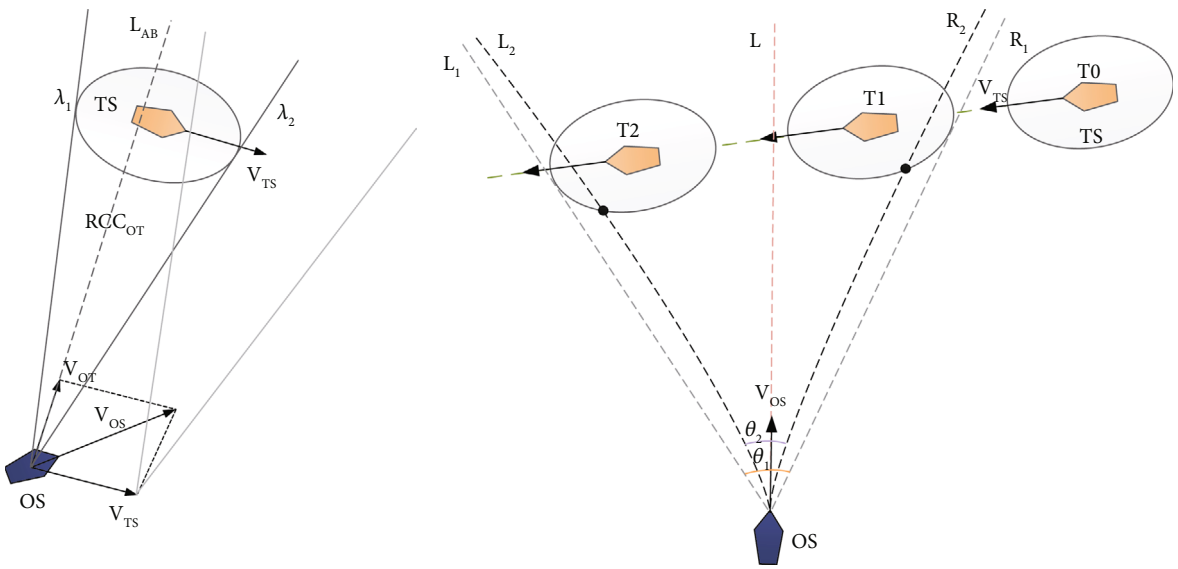

(a) Schematic diagram of the VO

(b) VO method considering ship manoeuverability

Figure 7: Illustration of VO method.

collision risk values can be therefore calculated by using the following functions:

$$CRI = a_i + \frac{\sigma_i^* - 0.2}{0.6 - 0.2} * (b_i - a_i). \tag{8}$$

3. Method for Ship Collision Avoidance

Due to the characteristics of ship motion such as large inertia, time delay, and nonlinear, ship manoeuvrability has a very important impact on the safety of ship navigation and the process of ship collision avoidance. It is necessary to establish a ship motion model to describe the nonlinear motion in the process of ship steering to avoid collision. Based on this, this section proposes an autonomous collision avoidance model based on the improved VO algorithm and the ship manoeuvring motion model. After calculating the course altering angle, the classical PID control model is used to control the ship steering. The autonomous collision avoidance model constructed in this paper is introduced below.

3.1. Course Control System. To accurately describe the ship manoeuvring motion in the process of collision avoidance, this study adopts the classic three-degree-of-freedom manoeuvring modeling group (MMG). The standardized 3-DOF MMG model is as follows:

$$\begin{cases} (m + m_x)\dot{u} - (m + m_y)v_m r - x_G m r^2 = X_H + X_R + X_P, \\ (m + m_y)\dot{v}_m - (m + m_x)ur - x_G m\dot{r} = Y_H + Y_R, \\ (I_z G + x_G^2 m + J_z)\dot{r} + x_G m(\dot{v}_m + ur) = N_H + N_R, \end{cases} \tag{9}$$

where m, m_x, and m_y, respectively, indicate the total mass of the vessel and additional mass in the vertical and horizontal axis directions. u, v, and v_m are surge velocity, lateral velocity at center of attractive, and lateral velocity at midship. X, Y, and N are hydrodynamic forces in the vertical and horizontal axis directions and altering moment. H, R, and P represent the force or moment of the hull, propeller, and rudder, respectively. The specific hydrodynamic coefficient and solution method can be referred to Yasukawa and Yoshimura [44]. The detailed particulars of the ship model follow the reference [39]. Classical PID control method is a kind of linear control, which combines the proportion (P), integral (I), and differential (D) of the deviation between the given value and the actual output value to form a control quantity through linear combination to control the controlled object. With the advantages of simple algorithm, high robustness, and strong reliability, it is very suitable for the control system with accurate mathematical model. Therefore, this paper adopts the classical PID control model to realize the ship course control. The PID controller is described as

$$u(t) = K_p e(t) + K_i \int_0^t e(t)dt + K_d \frac{de(t)}{dt}, \tag{10}$$

where K_p, K_i, and K_d are the proportional parameter, integral parameter, and derivative parameter, respectively. $e(t)$ is the system error signal and $u(t)$ is the output of the PID.

Discretizing Equation (10), the discrete form of PID controller is written as

$$u(s) = K_p e(s) + K_i T \sum_{s=0}^{m} e(s) + \frac{K_d}{T}[e(s) - e(s) - 1], \tag{11}$$

where T is the sampling period and m is the total number of sampling times.

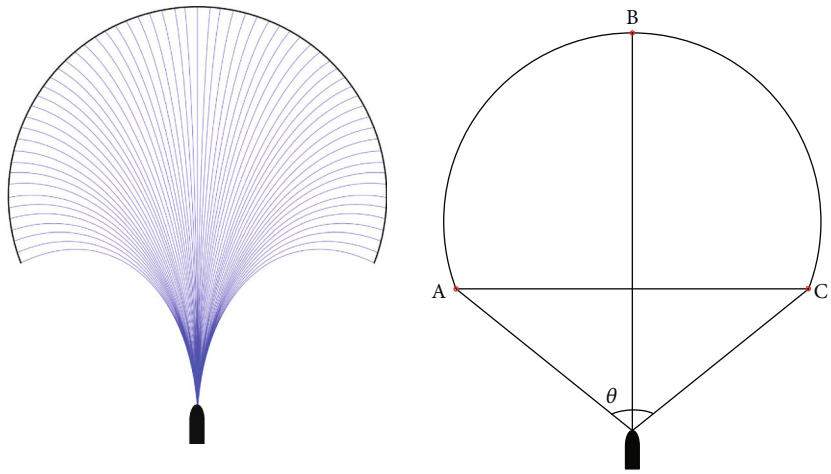

(a) Sets of ship trajectories over a period of time (b) Sets of ship trajectory after abstraction

Figure 8: Sets of trajectories of the ship's manoeuvring motion.

3.2. Collision Avoidance Method. In this section, we propose a collision avoidance method based on the modified VO algorithm. This method comprehensively considers ship manoeuvrability, ordinary practice of seaman, and COLREGs to harmonize the actions in collision avoidance manoeuvres. Firstly, according to the VO algorithm and ship manoeuvrability, the feasible velocity set where the ship can safely avoid the TSs can be determined. Then, according to the encounter situation and the requirements of the COLREGs, an optimal steering angle is determined to realize the collision avoidance of the ship. For complex encounter scenarios of multiple ships, it can be decomposed into two-ship encounter situations and then make decisions according to the constructed collision avoidance model.

3.2.1. Velocity Obstacle Algorithm. Velocity obstacle (VO) algorithm is an effective and simple collision avoidance method, which is widely used in robot obstacle avoidance and ship collision avoidance. The principle of the VO method is shown in Figure 7(a), and the method of ship collision avoidance is given below.

Let P_R represents the relative position between OS and TS and V_{OT} represents the relative velocity between OS and TS. Then, the ray position after time t is

$$\lambda(P_R, V_{OT}) = \{P_R + V_{OT} \cdot t | t \geq 0\}. \quad (12)$$

Suppose that α represents a circular area with TS as the center and d_s as the radius. The relative collision cone of OS which is relative to TS is

$$RCC_{OT} = \{V_{OT} | \lambda(P_{OS}, V_{OT}) \cap \alpha \neq \varnothing\}. \quad (13)$$

Then, the RCC_{OT} can be converted into velocity obstacle region according to the absolute velocity set:

$$VO_{OT} = RCC_{OT} \otimes V_{TS} = \{V_{OS} | \lambda(P_{OS}, V_{OS}) \cap \alpha \neq \varnothing\}, \quad (14)$$

where operation $\otimes$ is the Minkowski addition. The purpose is to obtain the point set of two Euclidean spaces.

3.2.2. Design of Collision Avoidance Method. In this section, ship manoeuvrability is introduced into the VO model. The ship motion model (MMG) is used to deduce the movement trend of the ship within a certain period of time. According to the MMG model to predict the ship's motion state in a period of time, the composition area of all positions that the ship can reach in the specified time is the set of the ship's motion trajectory in time t. Figure 8(a) shows the set of trajectories of the ship's manoeuvring motion at time t. Figure 8(b) shows the set of reachable trajectories after the abstraction of the manoeuvring motion of the ship at time t. Point B in Figure 8(b) is the maximum distance that the ship can reach in time t by maintaining the current speed and heading, and A and C are the maximum distance that the ship can reach in time t by taking the maximum rudder angle. θ is the feasible range of collision avoidance angle.

Therefore, ship manoeuvrability factor ρ is introduced and integrated into set $\{K_{VO} | \rho \in K_{VO}\}$. The set K_{VO} is a bounded set with constant upper bound, so the new velocity obstacle region can be obtained as follows:

$$V_{OT} = VO_{OT} \otimes K_{VO}. \quad (15)$$

Then, formula (15) is equivalent to the following formula:

$$V_{OT} = \{V_{OS} | \lambda(P_{OS}, V_{OS}) \rho \cap \alpha \neq \varnothing\}, \quad (16)$$

where $\otimes$ is the mathematical operators. ρ can be obtained from the simulation experiment of ship manoeuvrability.

Figure 7(b) is the schematic representation of the VO without considering the ship manoeuvrability and considering the ship manoeuvrability, respectively. In this case, when the TS exists, the critical angle of the OS is θ_2, which is smaller than the original critical angle (θ_1). Among them,

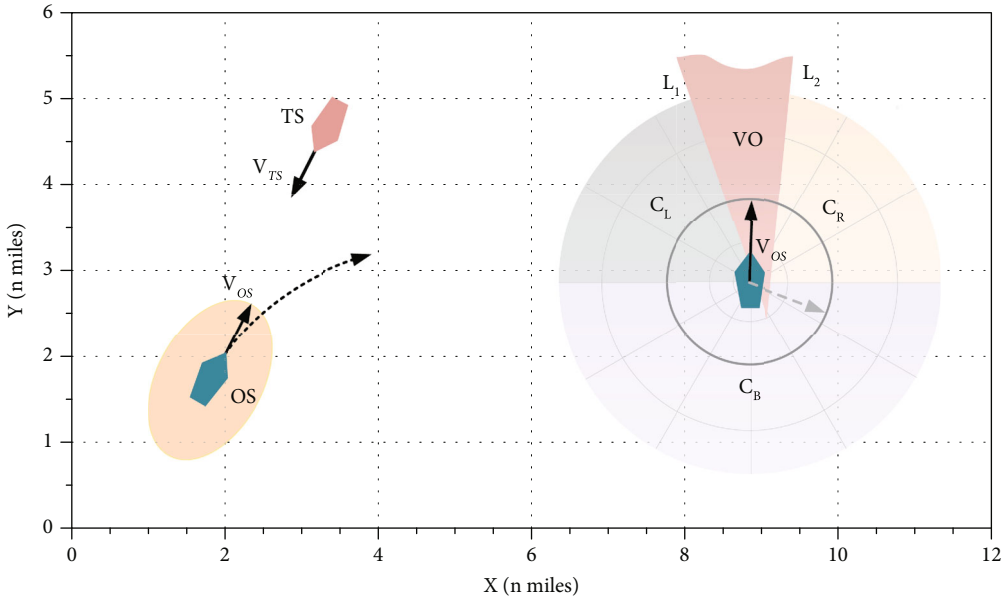

Figure 9: The diagram of collision avoiding in head-on situation.

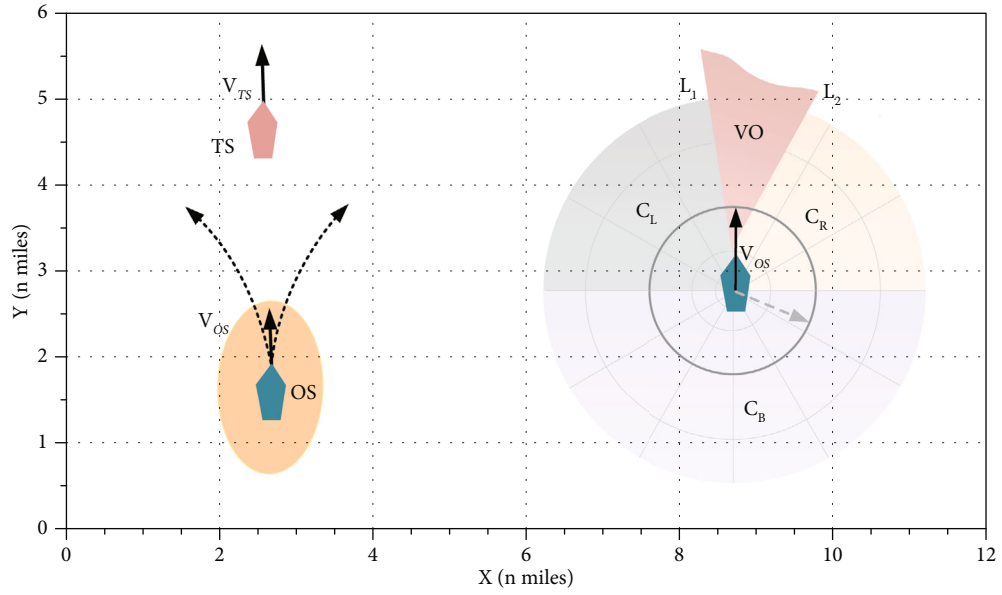

Figure 10: The diagram of collision avoiding in overtaking situation.

L2 (L1) and R2 (R1) are the left (original) boundary line and the right (original) boundary line of the OS, respectively.

Considering COLREGs and ordinary practice of seaman, reachable collision-free velocity sets under different encounter situations are constructed as follows:

Head-on situation: as shown in Figure 9, taking the OS as the center, the velocity reachable set is divided into four parts (same as Figures 10 and 11): VO set (light pink area), C_L set (light grey area), C_R set (light yellow area), and C_B set (light blue area). Based on the requirements of the ordinary practice of seaman, the ship's reversing manoeuver is not considered, so C_B set will not be used as an alternate avoidance area. According to rule 14 of COLREGs and the ordinary practice of seaman, the ship usually adopts a steering strategy to avoid collision in head-on situation. So, reachable collision-free velocity set is

$$C_{VO}^{H} = \{v | v \in C_R, v \notin V_{OT}\}. \tag{17}$$

Overtaking situation: for overtaking situations, OS may choose to overtake from the port or starboard side of TS according to COLREGs rule 13. However, the rules do not specify which side to overtake. As shown in Figure 10, in the overtaking situation, when the velocity of the OS falls into the VO set (light pink area), the OS will alter course to starboard or port side to avoid collision. So, reachable

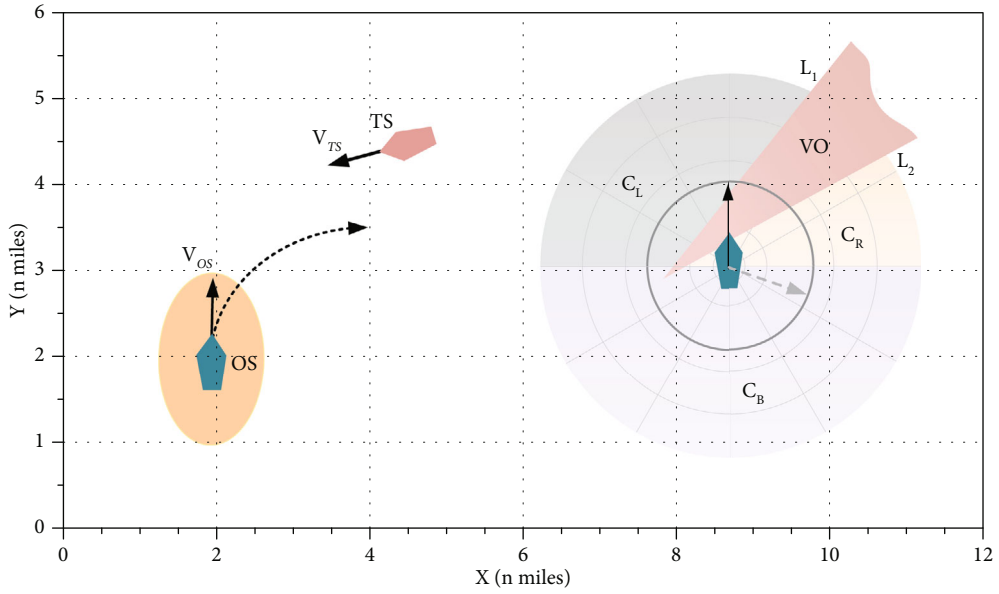

Figure 11: The diagram of collision avoiding in crossing situation.

collision-free velocity set is

$$C_{VO}^{O} = \{v | v \in C_L \cup C_R, v \notin V_{OT}\}. \quad (18)$$

Crossing situation: crossing encounter is generally divided into crossing on starboard side encounter and crossing on port side encounter. Considering that the purpose of this article is to study the OS as a give-way ship, this study only discusses the crossing on starboard side encounter scenarios, and crossing on port side encounter scenarios will be studied in the future. According to COLREGs rule 15, OS is a give-way ship when TS crossing on her starboard side, and she should alter course to starboard side to avoid collision. When OS's velocity falls in the VO set (light pink area), the OS should take collision avoidance action to starboard side, as shown in Figure 11. So, reachable collision-free velocity set is

$$C_{VO}^{C} = \{v | v \in C_R, v \notin V_{OT}\}. \quad (19)$$

Theoretically, any course altering angle within the collision-free VO set can make the giving-way ship safely avoid all TSs. However, considering the safety and economy in navigation, the course altering angle should not be too large or too small, so it is very necessary to choose an appropriate course altering angle. Based on this, this study introduces the safety parameter ξ; the optimum course steering angle θ of ship collision avoidance can be expressed by

$$\theta = \xi * \min \|C_{VO}\|, \quad (20)$$

where $\|C_{VO}\|$ represents the minimum value of reachable collision-free velocity sets and ξ always lies between 1.2 and 1.6, which can be adjusted according to specific circumstances.

3.3. Methodology Flow. On the basis of the collision detection model, collision risk evaluation model, and the modified VO method, the ship collision avoidance method is developed. This section gives the specific procedure for collision avoidance decision optimization method, which consists of 4 steps:

S1: collect ship parameter information, determine collision assessment area, and judge collision risk. The typical VO algorithm is used to judge whether there is a collision risk for ships in the PCA

S2: collision risk assessment. A novel CRA model based on the AGC is proposed for different encounter situations. This collision risk assessment method can realize the identification and quantification of ship collision risk in different encounter situations

S3: obtain the feasible VO set that allows all obstacles to be clear. Based on this, calculate the optimal steering angle of ship collision avoidance based on the modified VO algorithm

S4: determine the target course of the avoidance collision according to step 3, and control the ship's steering through the course control system

4. Case Study

In this section, simulation experiments are carried out to show the feasibility and effectiveness of the proposed collision avoidance method in various encounter scenarios.

4.1. Scenario Settings. In this section, to begin with, an area near Zhoushan Port in China for the case study is chosen; the real-time traffic density of ships is displayed in Figure 12. It can be seen that ship encountering situations occur frequently in the study area. In this study, the threshold value CRI_P is set to 0.70. The initial conditions include the ship position, ship speed, ship course, and ship distance of the ships. T_0, T_1, and T_2 are the start time, the middle time, and the end

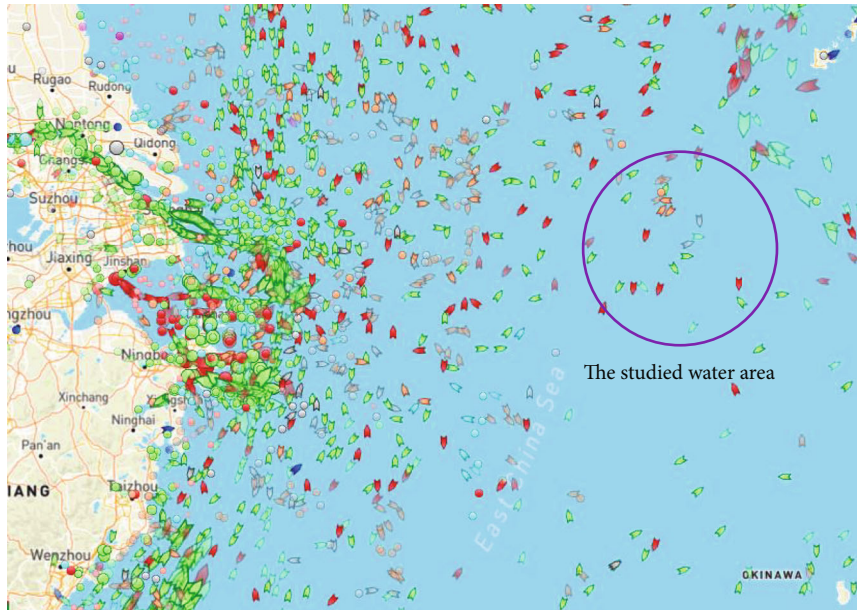

Figure 12: The water area selected for validation.

Table 5: The initial information and risk results of ships.

Number	Position	Course (deg)	True bearing (deg)	Speed (kn)	Distance (nm)	Collision risk	CRI
OS	29°57.768′N, 123°34.386′E	020.0	0	12	0	—	
TS1	30°1.764′N, 123°35.376′E	180.0	15.97	9	3.116	Yes	0.721
TS 2	29°55.44′N, 123°36.348′E	320.0	152.94	10	3.741	No	—
TS 3	29°54.696′N, 123°31.584′E	018.0	157.34	15	4.746	No	—
TS 4	29°57.258′N, 123°39.588′E	340.0	108.52	15	4.757	Yes	0.658
TS 5	30°1.362′N, 123°32.172′E	125.0	323.51	15	3.226	No	—

time during the collision avoidance process, respectively. D_{min} is the minimum distance between the two ships. In addition, it should be noted that in the graphs of simulation results, the solid red lines and dashed red lines denote the actual route and planned route of the OS during collision avoidance and the dashed other color lines and solid other color lines denote the planned route and actual route of TSs. The ellipse graphics represent the OS's ship domain, and the arrow represents the velocity vector lines of the ships. To validate the feasibility and effectiveness of the collision avoidance method proposed in this paper, both the single ship scenario (head-on, overtaking, and crossing encounter situation) and multiship scenario were selected as experimental scenarios.

4.2. Simulation Examples. In this section, the first is collecting ship parameter information and judging collision risk. In the PCA, the initial information of ships is shown in Table 5. The collision risk of each TSs is calculated by the collision detection model in Section 2.2, the results are shown in Table 5. Through the last column in Table 5, it can be found that TS1 and TS4 have collision risk with OS, while other TSs do not have collision risk with OS.

Then, the CRA model proposed in this paper is used to realize the identification and quantification of ship collision risk in different encounter situations. In the last part, when the CRI of the two ships exceeds the threshold, the collision avoidance model is triggered. Since the purpose of this paper is to verify the feasibility and effectiveness of the ship avoidance collision decision method, therefore, we select three different encounter situations and multiship separately based on Section 2 to verify the collision avoidance method proposed. In the next section, simulation experiments of ship collision avoidance method in various encounter scenarios are given when collision risk exists and exceeds the threshold.

4.2.1. Scenario 1: Head-On Situation. The first scenario is a head-on situation to demonstrate the performance of the proposed collision avoidance model. The basic information of simulation ships is shown in Table 6. The initial speed of the OS and TS are 12 kn and 10 kn, respectively. The coordinates are expressed in the distance; for the convenience of the simulation experiment, the unit is converted to kilometers (km).

Table 6: Initial information of the ships for head-on situation.

Ship list	Position (deg)	Course (°)	Speed (kn)	Distance (nm)	CRI
OS	29°59.082′N, 123°34.758′E	019.5	12	0	0.752
TS	30°1.644′N, 123°35.826′E	200	10	2.725	

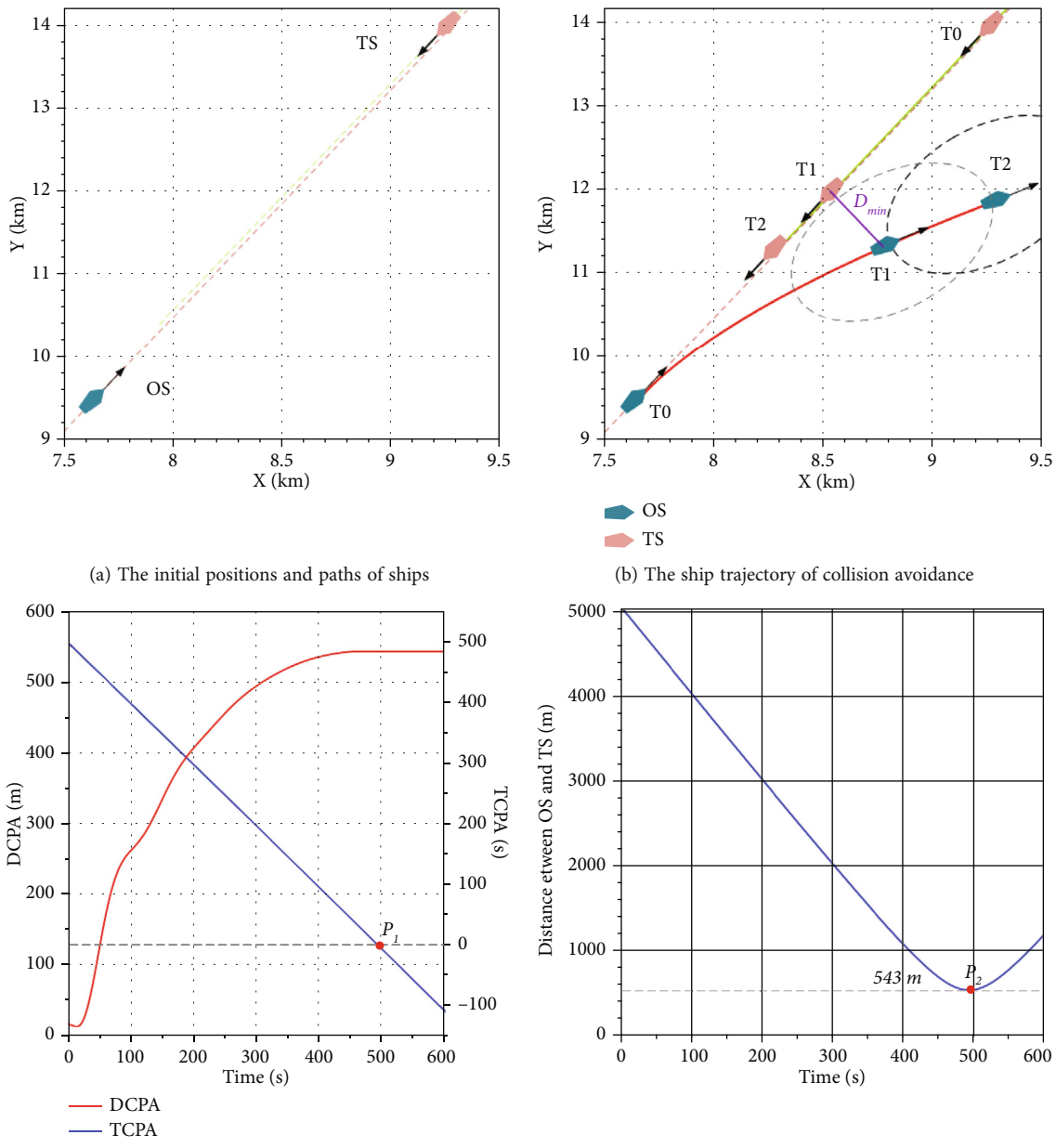

(a) The initial positions and paths of ships

(b) The ship trajectory of collision avoidance

(c) The DCPA/TCPA between OS and TS

(d) The relative distance between OS and TS

Figure 13: The simulation results under head-on encounter situation.

Table 7: Initial information of the ships for overtaking situation.

Ship list	Position (deg)	Course (°)	Speed (kn)	Distance (nm)	CRI
OS	29°58.806′N, 123°36.204′E	030	15	0	0.768
TS	30°0.510′N, 123°37.458′E	030	6	2.022	

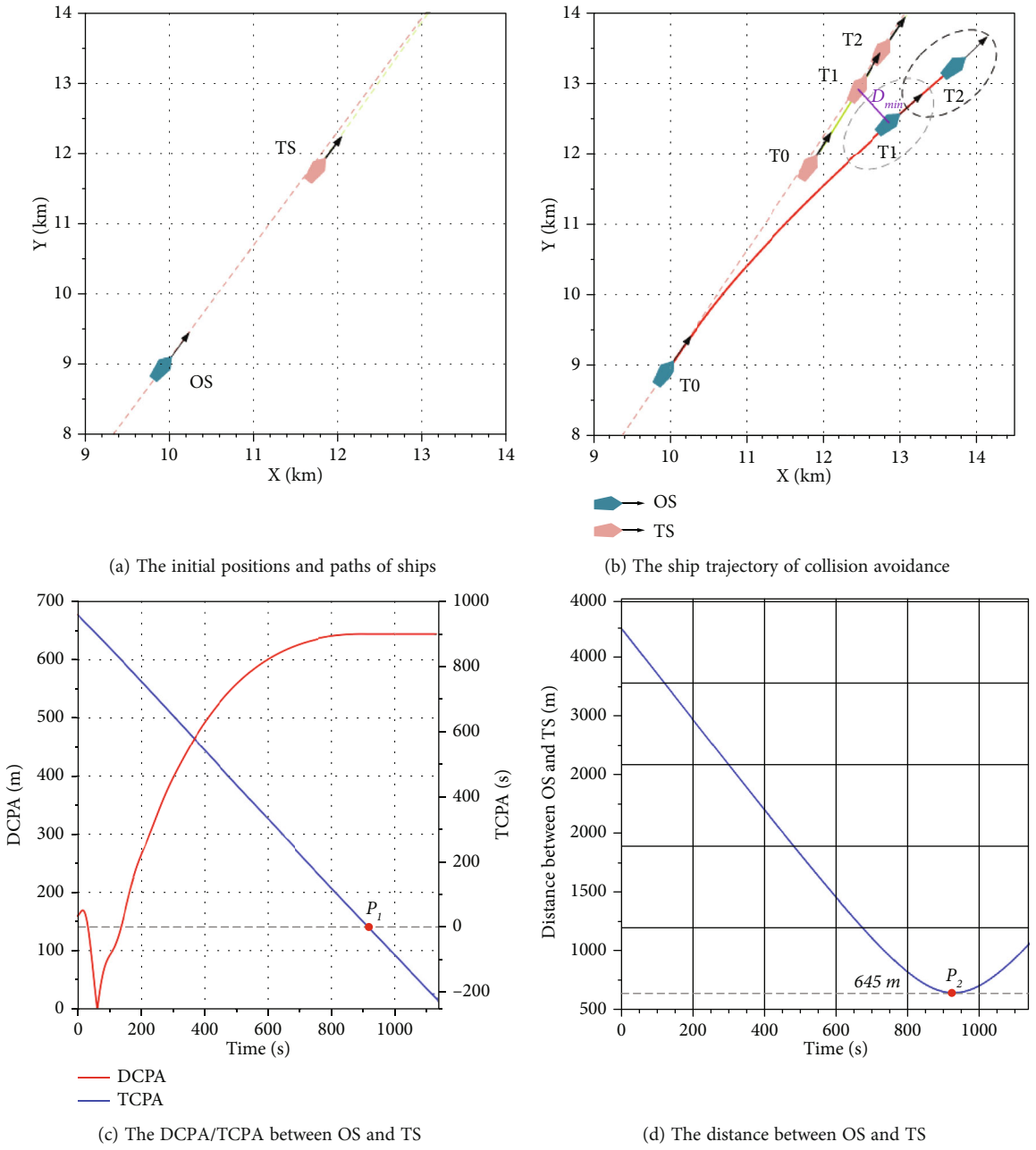

(a) The initial positions and paths of ships

(b) The ship trajectory of collision avoidance

(c) The DCPA/TCPA between OS and TS

(d) The distance between OS and TS

Figure 14: The simulation results under overtaking encounter situation.

Table 8: Initial information of the ships for crossing situation.

Ship list	Position (deg)	Course (°)	Speed (kn)	Distance (nm)	CRI
OS	30°0.324′N, 123°39.942′E	120	15	0	0.744
TS	29°58.362′N, 123°41.370′E	345	13	2.321	

In the current encounter situation, the collision avoidance model is activated when the value of CRI exceeds the threshold. According to the COLREGs, the OS should actively alter course to starboard side for collision avoidance. Assuming that the TS's actions are proactive, the collision avoidance operation is performed by the OS alone.

Figure 13 shows the simulation results under head-on encounter situation. Figures 13(a) and 13(b) show the positions and paths at the initial time, middle time, and end time in the process of collision avoidance. The changes of DCPA, TCPA, and D between two ships during the entire collision avoidance manoeuvres are shown

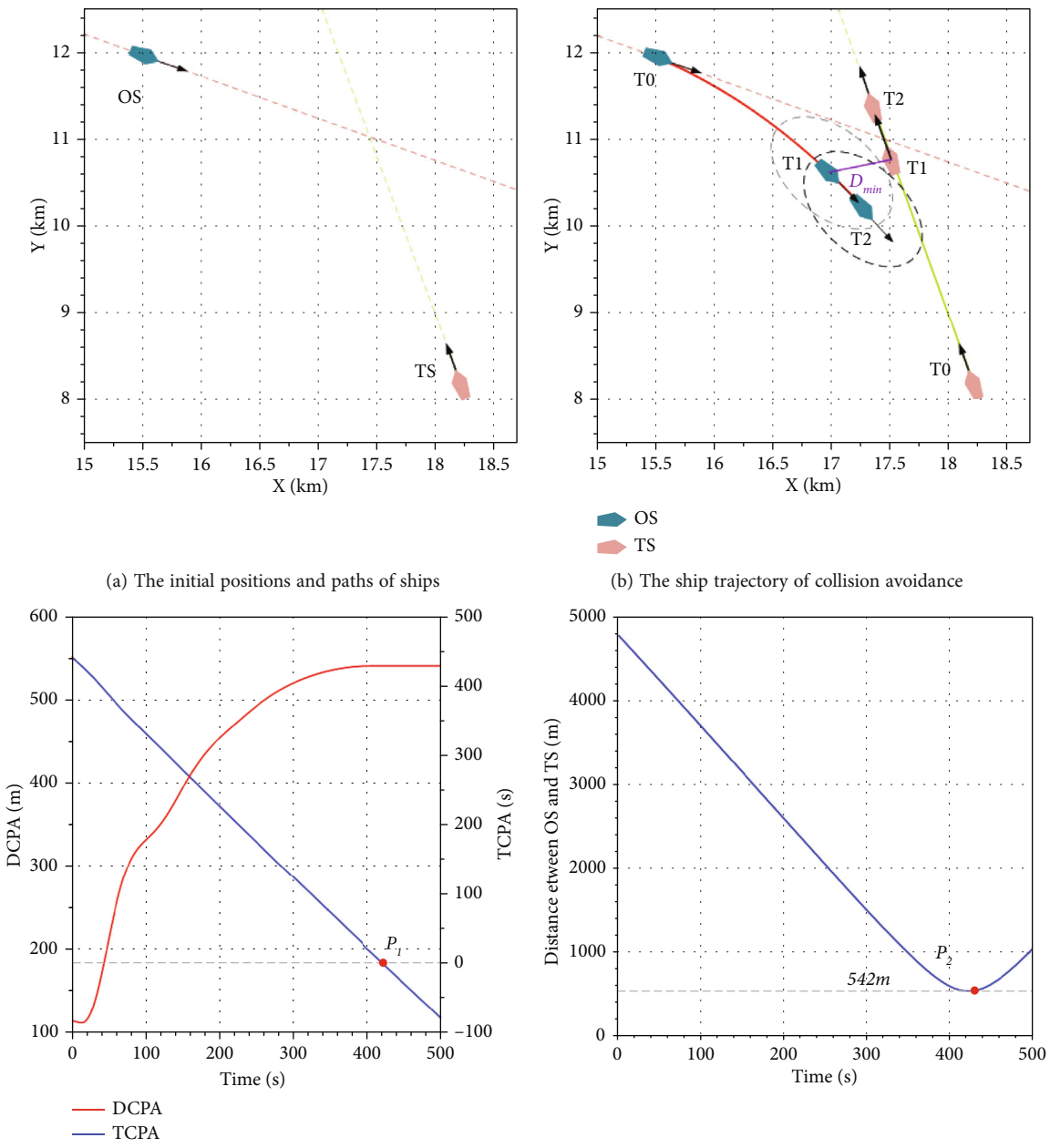

(a) The initial positions and paths of ships

(b) The ship trajectory of collision avoidance

(c) The DCPA/TCPA between OS and TS

(d) The relative distance between OS and TS

Figure 15: The simulation results under crossing encounter situation.

Table 9: Initial information of the ships for multiship situation.

Ship list	Position	Course (°)	Speed (kn)	Distance (nm)	CRI
OS	29°59.259′N, 123°32.918′E	000	12	0	—
TS1	30°3.914′N, 123°30.55′E	140	12	5.063	0.712
TS2	29°59.353′N, 123°31.337′E	040	10	1.367	0.548
TS3	30°4.983′N, 123°41.364′E	180	10	5.834	0.675
TS4	30°3.531′N, 123°35.267′E	210	12	4.634	0.707

in Figures 13(c) and 13(d). From the ship trajectory and experimental results, an explanation of the collision avoidance process is as follows.

As shown in Figure 13(a), the OS and TS are in a head-on situation. The collision avoidance parameter information at this time is shown in Table 6. At this time, the value of

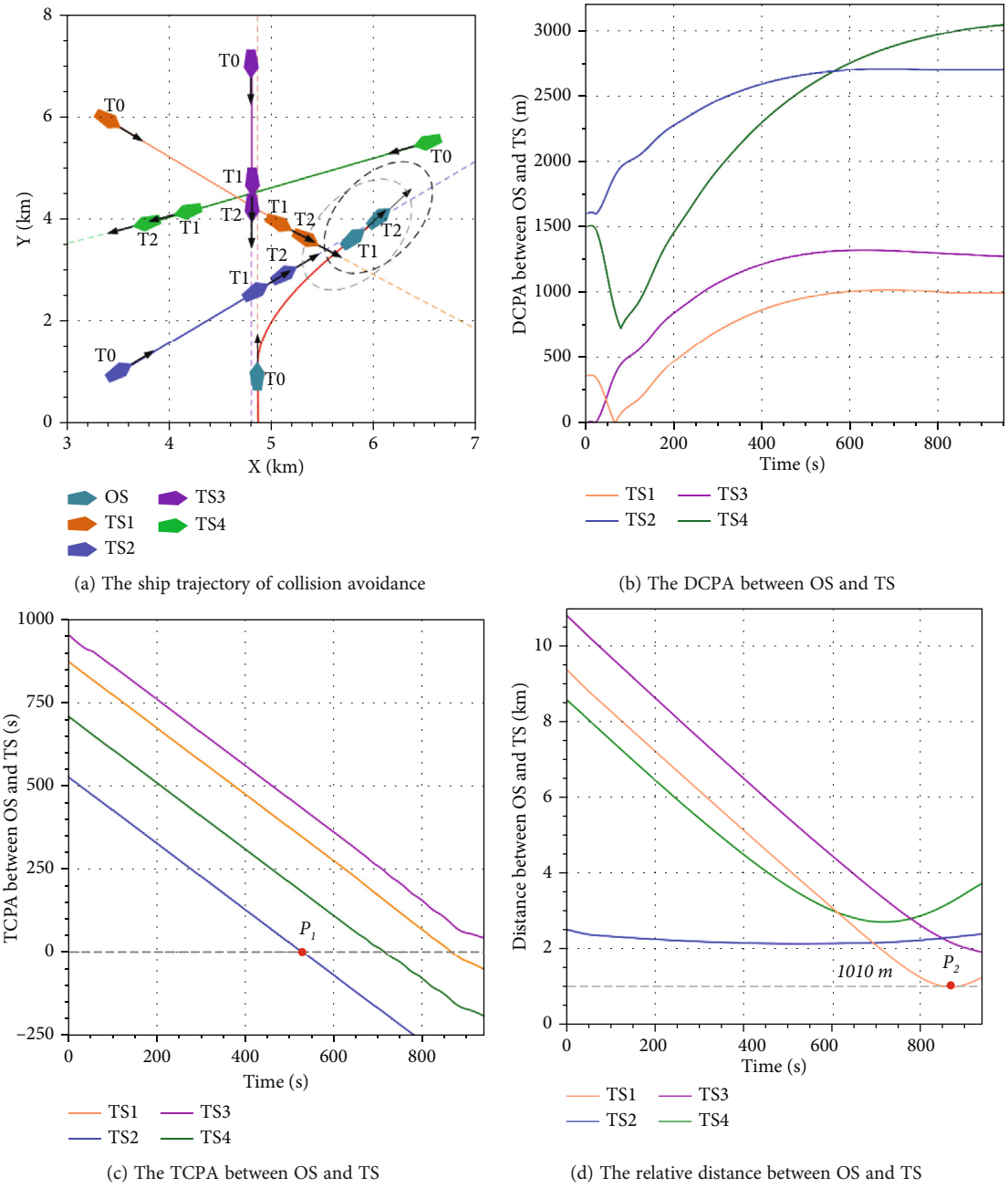

Figure 16: The simulation results under multiship encounter situation.

Table 10: Collision avoidance information of simulation results.

Case	Φ	θ (°)	$T_{TCPA=0}$ (s)	D_{min} (m)
Case 1	Turn to starboard	25	495	543
Case 2	Turn to starboard	20	924	645
Case 3	Turn to starboard	30	422	542
Case 4	Turn to starboard	42	866, 530, 961, and 716	1010, 2153, 1900, and 2723

CRI is 0.752, and it is greater than the threshold value 0.7. Risk of collision exists in the current scene, so the collision avoidance model starts to be activated. According to the collision avoidance method, the OS makes the decision of turning 25° to starboard. When the OS is in the position T_1 as shown in Figure 13(b), the values of TCPA and CRI are gradually reduced which means the collision avoidance strategy is starting to work by taking the proper action. As

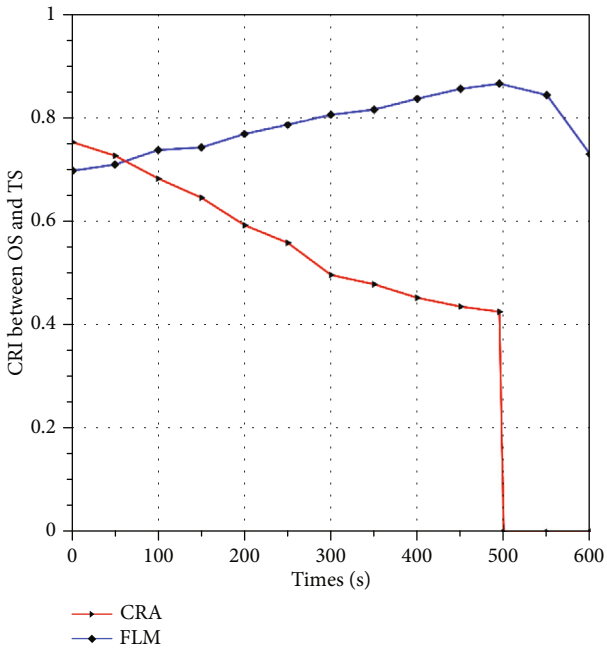

Figure 17: Comparison of CRA and FLM analysis results.

show in Figure 13(b), when $t = 601$ s (T_2), OS and TS are moving away. It shows that the collision avoidance manoeuver is effective. The change of DCPA and TCPA between OS and TS is shown in Figure 13(c). The TCPA values decrease gradually in the process of collision avoidance. The TCPA value of point P_1 is 0. The general tendency of DCPA values is increased. In Figure 13(d), the ship's relative distance curve gradually decreases first, reaching the lowest point of the curve at the point P_2 at 495 s, and the relative distance is 543 m and then gradually raises to around 1200 m. The results show that the collision avoidance manoeuver is effective and reliable.

4.2.2. Scenario 2: Overtaking Situation. In this scenario, the initial information of ships is shown in Table 7. For overtaking situations, OS may choose to overtake from the port or starboard side of TS according to COLREGs rule 13. However, the rules do not specify which side to overtake, considering the economy and safety of the ship's navigation, it is generally preferred to alter course to starboard side. The results of ship collision avoidance decisions and manoeuvres are shown in Figure 14.

Figure 14(a) shows the overtaking encounter situation. The OS is heading towards TS; if OS does not take collision avoidance manoeuvre, the two ships will collide. According to the COLREGs rule 13, the OS shall be fully responsible for avoiding conflict. The collision avoidance information to this moment is shown in Table 7. Accordingly, the OS began to avoid collision action. The OS should alter to starboard by 20°. It can be illustrated in Figure 14(b) that OS is overtaking TS from the port side. When $t = 926$ s (T_1), the distance of OS is closest to the TS, and it is 645 m. It shows that OS successfully handles the overtaking encounter by taking the collision avoidance decision. The changes of DCPA, TCPA, and D between OS and TS are shown in Figures 14(c) and 14(d). The TCPA values are decreased gradually during collision avoidance manoeuver. The general tendency of DCPA values is increased. The TCPA value of point P_1 is 0. The ship's relative distance curve gradually decreases first, reaching the lowest point of the curve at point P_2, and then gradually raises.

4.2.3. Scenario 3: Crossing Situation. The initial information of simulation ships is shown in Table 8. Figures 15(a) and 15(b) show the positions and trajectories of the simulation ships at several typical time points. The changes of DCPA, TCPA, and D between two ships during the entire collision avoidance manoeuvres are shown in Figures 15(c) and 15(d). The collision avoidance process is analyzed from the ship trajectory and experimental results as follows.

The collision avoidance parameter information at this time is shown in Table 8. At this point, CRI is greater than the threshold value 0.7. Accordingly, the OS begins to avoid collision action, and the OS makes the decision of turning 30° to starboard. When the OS is in the position (T_1) as shown in Figure 15(b), the values of TCPA are gradually reduced, and the DCPA values are increased. In Figure 15(d), the ship's relative distance curve gradually decreases at first, reaching the lowest point, and then gradually raises. When $t = 423$ s, the relative distance between OS and TS reaches the minimum value of 542 m. The results show that the collision avoidance manoeuver is effective.

4.2.4. Scenario 4: Multiship Situation. This scenario is a typical and complicated five-ship encounter situation. The initial information of simulation ships is shown in Table 9. In this scenario, TS1 and TS2 are located on the port side of the OS and form port side-crossing encounter situations with OS, respectively. TS3 is located at the port bow of the OS and forms a head-on situation with OS. TS4 is located on the starboard side and form starboard side-crossing encounter situations with OS. According to the collision detection model in Section 2.2, it can be known that the OS has a collision risk with TS1, TS2, TS3, and TS4, respectively. Multiship encounter situations can be decomposed into single encounter situations. The collision avoidance decision scheme is formulated to pass and clear all TSs with the risk of collision at one time. For the TS3 and TS4, the OS is a give-way ship. According to the collision avoidance model, OS can only clear all TSs by altering course 42° to starboard. Figure 15 shows the simulation results under multiship encounter situation.

Figure 16(a) shows the whole collision avoidance process of the simulated ships involved in the experiment. OS crosses from the starboard side of TS1 and TS2 and TS3 and TS4 cross from the port side of OS. It can be seen that when the OS is in the position T_1, all TSs are outside the ship domain of the OS. In other words, the minimum distance between the OS and each TS is greater than the required safe passing distance. The real-time collision avoidance parameter changes are shown in Figures 16(b)–16(d). As the OS takes the collision avoidance decisions, the overall trend of the DCPA values of the OS and TSs is to increase

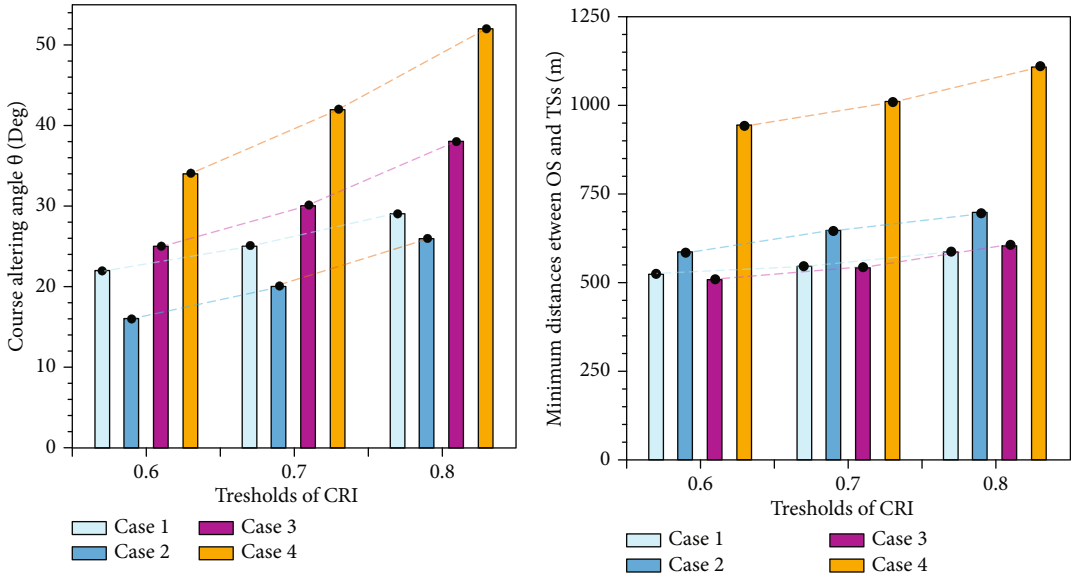

(a) The course altering angle θ

(b) The minimum distance between OS and TSs

Figure 18: Comparison of the results of different thresholds.

first and then stabilize. The TCPA values between OS and TSs change to negative at 867 s, 528 s, 908 s, and 720 s in Figure 16(c), respectively. Figure 16(d) shows the ship's relative distance curves between OS and TSs, which reaches the lowest point in 866 s, 530 s, 961 s, and 716 s, and the minimum distances are 1010 m, 2153 m, 1900 m, and 2723 m separately.

4.3. Analysis and Discussions. In the above cases, the collision avoidance method is tested by a series of simulation experiments. The simulation results show that the collision avoidance model can safely and reasonably handle the collision of ship in three typical single-ship encounter situations and multiship encounter situations and is summarized in Table 10, which gives the collision avoidance action Φ, course altering angle θ, $T_{\mathrm{TCPA}=0}$, and $D_{\min}$ values of TSs encountered by OS in each scenario.

In fact, in four cases, the OS alters to starboard by 25°, 20°, 30°, and 42° respectively, to avoid the TSs. The minimum relative distance for all scenarios is greater than the safe passing distance, which confirms that ship domain of OS is consistently not invaded by TSs. For all simulation scenarios, after collision avoidance is completed, the CRI values between OS and TSs are less than the threshold 0.7. In order to verify the effectiveness of the collision risk assessment model proposed in this paper, the optimization results of CRA model and traditional FLM are compared and analyzed. Taking the head-on situation as an example, the calculation results are shown in Figure 17. In Figure 17, by comparing the two evaluation models, it can be seen that in the process of ship collision avoidance, the collision risk value calculated by FLM gradually increases, reaches the maximum value at 495 s, and then gradually decreases. The value of collision risk calculated by CRA model constructed in this paper gradually decreases, and the value of collision risk of two ships is 0 after 495 s, which means no collision risk between two ships. Since ship manoeuverability is considered in the collision avoidance model constructed in this paper, the collision risk value begins to decrease gently after the ship begins to turn and avoid. After 495 s, the two ships are finally past and clear and there is no collision risk at this time, so the collision risk value is 0. It shows that the CRA model is more practical in solving the problem of ship collision risk, and it is reasonable to quantify the ship collision risk based on asymmetric grey cloud.

Considering that there are differences in the timing of ship collision avoidance under different encounter situations, different threshold values of the CRI are set in this paper. Figure 18 shows the parameters (course altering angle and minimum distance between OS and TSs) of the ships' action measures in the collision avoidance process under different thresholds (0.6, 0.7, and 0.8). Some studies have shown that when the threshold value is relatively little, the steering amplitude of collision avoidance is generally smaller. On the contrary, when the threshold is relatively large, the ships take larger steering actions [7]. The experiment has been tested that it is in line with the practical situation. According to the COLREGs, a series of small manoeuvers must be avoided. Taking excessive steering actions can easily cause the ship to deviate further from the original route. In general, different decision-makers may choose different thresholds. This is treated as reasonable.

In summary, compared with previous studies [45], the main contributions of this paper are mainly as follows. (1) A novel CRA model based on asymmetric AGC is proposed for different encounter situations, which can effectively consider the randomness, ambiguity, and incompleteness of the information in the ship collision risk evaluation process. (2) Based on the inherent good characteristics of the VO model, the collision avoidance model in this paper attempts to combine manoeuvring motion characteristics of vessels with a

modified VO algorithm. The ship collision avoidance model can consider various factors including ship manoeuvrability, ship encounter situation, navigation practice, and COLREGs. The collision avoidance method based on the CRA model and modified VO method improves the stability and reliability of the ship collision avoidance. Through a series of simulation results, it can be seen that the collision avoidance method proposed in this study has strong adaptability and feasibility and can deal with a variety of typical encounter scenarios, especially suitable for the decision-making process of ship collision avoidance in open waters. In addition, based on the manoeuvring motion characteristics of ship, the collision avoidance model can continuously update and output new collision avoidance decision schemes according to the current scene.

5. Summary and Conclusions

The main contribution of this paper is to present a novel real-time collision avoidance model for autonomous ships based on a modified VO algorithm and grey cloud model. The proposed collision detection method proposed in this paper, on one hand, can achieve real-time monitoring of ships in PCA. On the other hand, it is possible to effectively screen the ship with the collision risk and reduce the calculation workload of collision risk. A novel CRA model based on AGC is proposed for different encounter situations, which can effectively consider the randomness, ambiguity, and incompleteness of the information in the ship collision risk evaluation process. Finally, we put forward a deterministic collision avoidance decision-making model based on the modified VO algorithm and ship manoeuvrability. The ship manoeuvrability, ship encounter situation, ordinary practice of seaman, and COLREGs are comprehensively considered in this collision avoidance model. The simulation results show that the proposed CRA model can effectively identify and quantify the collision risk under different encounter situations in real time, collision avoidance model can realize ship collision avoidance under different encounter situations, and it has an important practical application value.

However, the collision avoidance model proposed in this paper does not consider the ship's variable speed decisions. The consideration of the decision of ship steering angle and variable ship speed, as well as to test the scene in a complex encounter situation, should be studied as a focus in the future.

Data Availability

The data that support the findings of this study are available from the corresponding author upon reasonable request.

Conflicts of Interest

No potential conflict of interest was reported by the authors.

Authors' Contributions

K.Z. conceptualized the study and assisted with methodology. K.Z. and X.Z provided the software. K.Z. and G.H. validated the study and participated in formal analysis. K.Z., C.X., and L.Z. assisted with data curation. K.Z. wrote the original draft. K.Z., L.H., L.Z., W.H., and G.H. wrote, reviewed, and edited the manuscript. K.Z., C.X., W.H., X.Z., and L.Z. contributed to visualization. L.H. and C.X. supervised the study. L.H. and G.H. carried out project administration. L.H made great contribution to funding acquisition. All authors have read and agreed to the published version of the manuscript.

Acknowledgments

This work is partially supported by the National Key Research and Development Program (Grant number 2019YFB1600603), the National Natural Science Foundation of China (Grant number 52071249), and the High-Tech Ship Research Projects sponsored by the MIIT-Green Intelligent Inland Ship Innovation Program of China (No. 2020YFE0201200).

References

[1] C. Zhao, R. Li, Y. Wang, H. Yu, and Y. Gong, "Study on the propagation of sustainable development concept among gulf ports based on complex network," *Maritime Policy & Management*, vol. 48, no. 4, pp. 478–496, 2021.

[2] C. Xie, L. Huang, R. Wang, J. Deng, Y. Shu, and D. Jiang, "Research on quantitative risk assessment of fuel leak of LNG-fuelled ship during lock transition process," *Reliability Engineering and System Safety*, vol. 221, article 108368, 2022.

[3] R. Szlapczynski and J. Szlapczynska, "A method of determining and visualizing safe motion parameters of a ship navigating in restricted waters," *Ocean Engineering*, vol. 129, pp. 363–373, 2017.

[4] EMSA, "Preliminary annual overview OF marine casualties and incidents 2014-2019," 2020, http://www.emsa.europa.eu/accident-investigation-publications/annual-overview.html.

[5] EMSA, "Annual overview of marine casualties and incidents 2020," 2020.

[6] M. Liang, R. W. Liu, S. Li, Z. Xiao, X. Liu, and F. Lu, "An unsupervised learning method with convolutional auto-encoder for vessel trajectory similarity computation," *Ocean Engineering*, vol. 225, article 108803, 2021.

[7] Y. Hu, A. Zhang, W. Tian, J. Zhang, and Z. Hou, "Multi-ship collision avoidance decision-making based on collision risk index," *Journal of Marine Science and Engineering*, vol. 8, no. 9, p. 640, 2020.

[8] Z. Liu, Z. Wu, and Z. Zheng, "An improved danger sector model for identifying the collision risk of encountering ships," *Journal of Marine Science and Engineering*, vol. 8, no. 8, 2020.

[9] R. Zhen, Z. Shi, J. Liu, and Z. Shao, "A novel arena-based regional collision risk assessment method of multi-ship encounter situation in complex waters," *Ocean Engineering*, vol. 246, article 110531, 2022.

[10] R. Szlapczynski and J. Szlapczynska, "Review of ship safety domains: models and applications," *Ocean Engineering*, vol. 145, pp. 277–289, 2017.

[11] R. Szlapczynski and J. Szlapczynska, "A ship domain-based model of collision risk for near-miss detection and collision alert systems," *Reliability Engineering and System Safety*, vol. 214, article 107766, 2021.

[12] R. Szlapczynski and J. Szlapczynska, "An analysis of domain-based ship collision risk parameters," *Ocean Engineering*, vol. 126, pp. 47–56, 2016.

[13] T. Brcko, A. Androjna, J. Srše, and R. Boć, "Vessel multi-parametric collision avoidance decision model: fuzzy approach," *Journal of Marine Science and Engineering*, vol. 9, no. 1, p. 49, 2021.

[14] W. Zhang, X. Feng, F. Goerlandt, and Q. Liu, "Towards a convolutional neural network model for classifying regional ship collision risk levels for waterway risk analysis," *Reliability Engineering and System Safety*, vol. 204, article 107127, 2020.

[15] N. Wang, "A novel analytical framework for dynamic quaternion ship domains," *Journal of Navigation*, vol. 66, no. 2, pp. 265–281, 2013.

[16] S. Wang, Y. Zhang, and L. Li, "A collision avoidance decision-making system for autonomous ship based on modified velocity obstacle method," *Ocean Engineering*, vol. 215, article 107910, 2020.

[17] A. S. Lenart, "Collision threat parameters for a new radar display and plot technique," *Journal of Navigation*, vol. 36, no. 3, pp. 404–410, 1983.

[18] Y. Huang and P. H. A. J. M. van Gelder, "Time-varying risk measurement for ship collision prevention," *Risk Analysis*, vol. 40, no. 1, pp. 24–42, 2020.

[19] P. Chen, Y. Huang, E. Papadimitriou, J. Mou, and P. H. A. J. M. van Gelder, "An improved time discretized non-linear velocity obstacle method for multi-ship encounter detection," *Ocean Engineering*, vol. 196, article 106718, 2020.

[20] T. Cepowski, "The prediction of ship added resistance at the preliminary design stage by the use of an artificial neural network," *Ocean Engineering*, vol. 195, article 106657, 2020.

[21] L. Zhang, J. Mou, P. Chen, and M. Li, "Path planning for autonomous ships: a hybrid approach based on improved apf and modified vo methods," *Journal of Marine Science and Engineerings*, vol. 9, no. 7, 2021.

[22] Y. Huang, L. Chen, and P. H. A. J. M. van Gelder, "Generalized velocity obstacle algorithm for preventing ship collisions at sea," *Ocean Engineering*, vol. 173, p. 142, 2019.

[23] Y. Huang, P. H. A. J. M. Van Gelder, and Y. Wen, "Velocity obstacle algorithms for collision prevention at sea," *Ocean Engineering*, vol. 151, p. 308, 2018.

[24] P. F. Chen, P. H. A. J. M. van Gelder, and J. M. Mou, "Integration of elliptical ship domains and velocity obstacles for ship collision candidate detection," *TransNav: International Journal on Marine Navigation and Safety of Sea Transportation*, vol. 13, no. 4, pp. 751–758, 2019.

[25] J. Li, H. Wang, W. Zhao, and Y. Xue, "Ship's trajectory planning based on improved multiobjective algorithm for collision avoidance," *Journal of Advanced Transportation*, vol. 2019, Article ID 4068783, 12 pages, 2019.

[26] T. Praczyk, "Neural anti-collision system for autonomous surface vehicle," *Neurocomputing*, vol. 149, pp. 559–572, 2015.

[27] S. Xie, X. Chu, M. Zheng, and C. Liu, "Ship predictive collision avoidance method based on an improved beetle antennae search algorithm," *Ocean Engineering*, vol. 192, article 106542, 2019.

[28] H. Lyu and Y. Yin, "COLREGS-constrained real-time path planning for autonomous ships using modified artificial potential fields," *Journal of Navigation*, vol. 72, no. 3, pp. 588–608, 2019.

[29] Y. Huang, L. Chen, R. R. Negenborn, and P. H. A. J. M. Van Gelder, "A ship collision avoidance system for human-machine cooperation during collision avoidance," *Ocean Engineering*, vol. 217, article 107913, 2020.

[30] S. Xie, V. Garofano, X. Chu, and R. R. Negenborn, "Model predictive ship collision avoidance based on Q-learning beetle swarm antenna search and neural networks," *Ocean Engineering*, vol. 193, article 106609, 2019.

[31] H. Shen, H. Hashimoto, D. Terada, and C. Guo, "Automatic collision avoidance of multiple ships based on deep Q-learning," *Applied Ocean Research*, vol. 86, pp. 268–288, 2019.

[32] J. Woo and N. Kim, "Collision avoidance for an unmanned surface vehicle using deep reinforcement learning," *Ocean Engineering*, vol. 199, article 107001, 2020.

[33] J. H. Ahn, K. P. Rhee, and Y. J. You, "A study on the collision avoidance of a ship using neural networks and fuzzy logic," *Applied Ocean Research*, vol. 37, pp. 162–173, 2012.

[34] L. Zhao, M. Il Roh, and S. J. Lee, "Control method for path following and collision avoidance of autonomous ship based on deep reinforcement learning," *Journal of Marine Science and Technology*, vol. 27, no. 4, pp. 293–310, 2019.

[35] X. Zhang, C. Wang, L. Jiang, L. An, and R. Yang, "Collision-avoidance navigation systems for maritime autonomous surface ships: a state of the art survey," *Ocean Engineering*, vol. 235, article 109380, 2021.

[36] Y. Hu, X. Meng, Q. Zhang, and G. K. Park, "A real-time collision avoidance system for autonomous surface vessel using fuzzy logic," *IEEE Access*, vol. 8, pp. 108835–108846, 2020.

[37] X. Wu, K. Liu, J. Zhang, Z. Yuan, J. Liu, and Q. Yu, "An optimized collision avoidance decision-making system for autonomous ships under human-machine cooperation situations," *Journal of Advanced Transportation*, vol. 2021, Article ID 7537825, 17 pages, 2021.

[38] Y. He, Y. Jin, L. Huang, Y. Xiong, P. Chen, and J. Mou, "Quantitative analysis of COLREG rules and seamanship for autonomous collision avoidance at open sea," *Ocean Engineering*, vol. 140, pp. 281–291, 2017.

[39] Y. T. Kang, W. J. Chen, D. Q. Zhu, and J. H. Wang, "Collision avoidance path planning in multi-ship encounter situations," *Journal of Marine Science and Technology*, vol. 26, no. 4, pp. 1026–1037, 2021.

[40] H. L. Wang, "Grey cloud model and its application in intelligent decision support system supporting complex decision," in *Proceedings - ISECS International Colloquium on Computing, Communication, Control, and Management, CCCM 2008*, vol. 1, pp. 542–546, Guangzhou, China, 2008.

[41] D. Luo, L. Ye, and D. Sun, "International Journal of Disaster Risk Reduction Risk evaluation of agricultural drought disaster using a grey cloud clustering model in Henan province, China," *International Journal of Disaster Risk Reduction*, vol. 49, article 101759, 2020.

[42] F. Wang, X. Liang, C. Guo, and P. Li, "Guidance simulation credibility evaluation based on clustering with grey cloud and entropy weight," *Journal of System Simulation*, vol. 27, no. 8, pp. 1703–1707, 2015.

[43] M. Zhang, J. Montewka, T. Manderbacka, P. Kujala, and S. Hirdaris, "A big data analytics method for the evaluation of ship - ship collision risk reflecting hydrometeorological conditions," *Reliability Engineering and System Safety*, vol. 213, article 107674, 2021.

[44] H. Yasukawa and Y. Yoshimura, "Introduction of MMG standard method for ship maneuvering predictions," *Journal of Marine Science and Technology*, vol. 20, no. 1, pp. 37–52, 2015.

[45] K. Zhang, L. Huang, X. Liu et al., "A novel decision support methodology for autonomous collision avoidance based on deduction of manoeuvring process," *Journal of Marine Science and Engineering*, vol. 10, no. 6, p. 765, 2022.